Cat Head Detection - How to Effectively Exploit Shape and Texture Features

Weiwei Zhang[1], Jian Sun[1], and Xiaoou Tang[2]

[1] Microsoft Research Asia, Beijing, China
{weiweiz, jiansun}@microsoft.com
[2] Dept. of Information Engineering, The Chinese University of Hong Kong, Hong Kong
xtang@ie.cuhk.edu.hk

Abstract. In this paper, we focus on the problem of detecting the head of cat-like animals, adopting cat as a test case. We show that the performance depends crucially on how to effectively utilize the shape and texture features jointly. Specifically, we propose a two step approach for the cat head detection. In the first step, we train two individual detectors on two training sets. One training set is normalized to emphasize the shape features and the other is normalized to underscore the texture features. In the second step, we train a joint shape and texture fusion classifier to make the final decision. We demonstrate that a significant improvement can be obtained by our two step approach. In addition, we also propose a set of novel features based on oriented gradients, which outperforms existing leading features, e. g., Haar, HoG, and EoH. We evaluate our approach on a well labeled cat head data set with 10,000 images and PASCAL 2007 cat data.

1 Introduction

Automatic detection of all generic objects in a general scene is a long term goal in image understanding and remains to be an extremely challenging problem duo to large intra-class variation, varying pose, illumination change, partial occlusion, and cluttered background. However, researchers have recently made significant progresses on a particularly interesting subset of object detection problems, face [14, 18] and human detection [1], achieving near 90% detection rate on the frontal face in real-time [18] using a boosting based approach. This inspires us to consider whether the approach can be extended to a broader set of object detection applications.

Obviously it is difficult to use the face detection approach on generic object detection such as tree, mountain, building, and sky detection, since they do not have a relatively fixed intra-class structure like human faces. To go one step at a time, we need to limit the objects to the ones that share somewhat similar properties as human face. If we can succeed on such objects, we can then consider to go beyond. Naturally, the closest thing to human face on this planet is animal head. Unfortunately, even for animal head, given the huge diversity of animal types, it is still too difficult to try on all animal heads. This is probably why we have seen few works on this attempt.

In this paper, we choose to be conservative and limit our endeavor to only one type of animal head detection, cat head detection. This is of course not a random selection.

(a) cat-like animal (b) cats

Fig. 1. Head images of animals of the cat family and cats.

Our motivations are as follows. First, cat can represent a large category of cat-like animals, as shown in Figure 1 (a). These animals share similar face geometry and head shape; Second, people love cats. A large amount of cat images have been uploaded and shared on the web. For example, 2,594,329 cat images had been manually annotated in flickr.com by users. Cat photos are among the most popular animal photos on the internet. Also, cat as a popular pet often appears in family photos. So cat detection can find applications in both online image search and offline family photo annotation, two important research topics in pattern recognition. Third, given the popularity of cat photos, it is easy for us to get training data. The research community does need large and challenging data set to evaluate the advances of the object detection algorithm. In this paper, we provide 10,000, well labeled cat images. Finally and most importantly, the cat head detection poses new challenges for object detection algorithm. Although it shares some similar property with human face so we can utilize some existing techniques, the cat head do have much larger intra-class variation than the human face, as shown in Figure 1 (b), thus is more difficult to detect.

Directly applying the existing face detection approaches to detect the cat head has apparent difficulties. First, the cat face has larger appearance variations compared with the human face. The textures on the cat face are more complicated than those on the human face. It requires more discriminative features to capture the texture information. Second, the cat head has a globally similar, but locally variant shape or silhouette. How to effectively make use of both texture and shape information is a new challenging issue. It requires a different detection strategy.

(a) (b) (c)

Fig. 2. Mean cat head images on all training data. (a) aligned by ears. More shape information is kept. (b) aligned by both eyes and ears using an optimal rotation+scale transformation. (c) aligned by eyes. More texture information is kept.

To deal with the new challenges, we propose a joint shape and texture detection approach and a set of new features based on oriented gradients. Our approach is a two step approach. In the first step, we individually train a shape detector and a texture detector to exploit the shape and appearance information respectively. Figure 2 illustrates our basic idea. Figure 2 (a) and Figure 2 (c) are two mean cat head images over all training images: one aligned by ears to make the shape distinct; the other is aligned to reveal the texture structures. Correspondingly, the shape and texture detectors are trained on two differently normalized training sets. Each detector can make full use of most discriminative shape or texture features separately. Based on a detailed study of previous image and gradient features, e.g., Haar [18], HoG [1], EOH [7], we show that a new set of carefully designed Haar-like features on oriented gradients give the best performance in both shape and texture detectors.

In the second step, we train a joint shape and texture detector to fuse the outputs of the above two detectors. We experimentally demonstrate that the cat head detection performance can be substantially improved by carefully separating shape and texture information in the first step, and jointly training a fusion classifier in the second step.

1.1 Related Work

Since a comprehensive review of the related works on object detection is beyond the scope of the paper, we only review the most related works here.

Sliding window detection vs. parts based detection. To detect all possible objects in the image, two different searching strategies have been developed. The sliding window detection [14, 12, 18, 1, 17, 15, 20] sequentially scans all possible sub-windows in the image and makes a binary classification on each sub-window. Viola and Jones [18] presented the first highly accurate as well as real-time frontal face detector, where a cascade classifier is trained by AdaBoost algorithm on a set of Haar wavelet features. Dalal and Triggs [1] described an excellent human detection system through training a SVM classifier using HOG features. On the contrary, the parts based detection [5, 13, 9, 6, 3] detects multiple parts of the object and assembles the parts according to geometric constrains. For example, the human can be modeled as assemblies of parts [9, 10] and the face can be detected using component detection [5].

In our work, we use two sliding windows to detect the "shape" part and "texture" part of the cat head. A fusion classifier is trained to produce the final decision.

Image features vs. gradient features. Low level features play a crucial role in the object detection. The image features are directly extracted from the image, such as intensity values [14], image patch [6], PCA coefficients [11], and wavelet coefficients [12, 16, 18]. Henry et al.[14] trained a neural network for human face detection using the image intensities in 20×20 sub-window. Haar wavelet features have become very popular since Viola and Jones [18] presented their real-time face detection system. The image features are suitable for small window and usually require a good photometric normalization. Contrarily, the gradient features are more robust to illumination changes. The gradient features are extracted from the edge map [4, 3] or oriented gradients, which mainly include SIFT [8], EOH [7], HOG [1], covariance matrix[17], shapelet [15], and edgelet [19]. Tuzel et al. [17] demonstrated very good results on human detection using the covariance matrix of pixel's 1st and 2nd derivatives and pixel position as features.

Shapelet [15] feature is a weighted combination of weak classifiers in a local region. It is trained specifically to distinguish between the two classes based on oriented gradients from the sub-window. We will give a detailed comparison of our proposed features with HOG and EOH features in Section 3.1.

2 Our Approach – Joint Shape and Texture Detection

The accuracy of a detector can be dramatically improved by first transforming the object into a canonical pose to reduce the variability. In face detection, all training samples are normalized by a rotation+scale transformation. The face is detected by scanning all sub-windows with different orientations and scales. Unfortunately, unlike the human face, the cat head cannot be well normalized by a rotation+scale transformation duo to the large intra-class variation.

In Figure 2, we show three mean cat head images over 5,000 training images by three normalization methods. In Figure 2 (a), we rotate and scale the cat head so that both eyes appear on a horizontal line and the distance between two ears is 36 pixels. As we can see, the shape or silhouette of the ears is visually distinct but the textures in the face region are blurred. In a similar way, we compute the mean image aligned by eyes, as shown in Figure 2 (c). The textures in the face region are visible but the shape of the head is blurred. In Figure 2 (b), we take a compromised method to compute an optimal rotation+scale transformation for both ears and eyes over the training data, in a least square sense. As expected, both ears and eyes are somewhat blurred.

Intuitively, using the optimal rotation+scale transformation may produce the best result because the image normalized by this method contains two kinds of information. However, the detector trained in this way does not show superior performance in our experiments. Both shape and texture information are lost to a certain degree. The discriminative power of shape features or texture features is hurt by this kind of compromised normalization.

2.1 Joint shape and texture detection

In this paper, we propose a joint shape and texture detection approach to effectively exploit the shape and texture features. In the *training phase*, we train two individual detectors and a fusion classifier:

1. Train a shape detector, using the aligned training images by mainly keeping the shape information, as shown in Figure 2 (a); train a texture detector, using the aligned training image by mainly preserving the texture information, as shown in Figure 2 (c). Thus, each detector can capture most discriminative shape or texture features respectively.
2. Train a joint shape and texture fusion classifier to fuse the output of the shape and texture detectors.

In the *detection phase*, we first run the shape and texture detectors independently. Then, we apply the joint shape and texture fusion classifier to make the final decision. Specifically, we denote $\{c_s, c_t\}$ as output scores or confidences of the two detectors, and $\{f_s, f_t\}$ as extracted features in two detected sub-windows. The fusion classifier is trained on the concatenated features $\{c_s, c_t, f_s, f_t\}$.

Using two detectors, there are three kinds of detection results: both detectors report positive at roughly the same location, rotation, and scale; only the shape detector reports positive; and only the texture detector reports positive. For the first case, we directly construct the features $\{c_s, c_t, f_s, f_t\}$ for the joint fusion classifier. In the second case, we do not have $\{c_t, f_t\}$. To handle this problem, we scan the surrounding locations to pick a sub-window with the highest scores by the texture detector, as illustrated in Figure 3. Specifically, we denote the sub-window reported by the detector as $[x, y, w, h, s, \theta]$, where (x, y) is window's center, w, h are width and height, and s, θ are scale and rotation level. We search sub-windows for the texture/shape detector in the range $[x \pm w/4] \times [y \pm h/4] \times [s \pm 1] \times [\theta \pm 1]$. Note that we use real value score of the texture detector and do not make 0-1 decision. The score and features of the picked sub-window are used for the features $\{c_t, f_t\}$. For the last case, we compute $\{c_s, f_s\}$ in a similar way.

To train the fusion classifier, 2,000 cat head images in the validation set are used as the positive samples, and 4,000 negative samples are bootstrapped from 10,000 non-cat images. The positive samples are constructed as usual. The key is the construction of the negative samples which consist of all incorrectly detected samples by either the shape detector or the texture detector in the non-cat images. The co-occurrence relationship of the shape features and texture features are learned by this kind of joint training. The learned fusion classifier is able to effectively reject many false alarms by using both shape and texture information. We use support vector machine (SVM) as our fusion classifier and HOG descriptors as the representations of the features f_s and f_t.

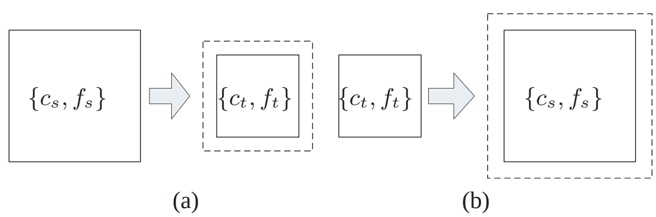

Fig. 3. Feature extraction for fusion. (a) given a detected sub-window (left) by the shape detector, we search a sub-window (right, solid line) with highest score by the texture detector in surrounding region (right, dashed line). The score and features $\{c_t, f_t\}$ are extracted for the fusion classifier. (b) similarly, we extract the score and features $\{c_s, f_s\}$ for the fusion.

The novelty of our approach is the discovery that we need to separate the shape and texture features and how to effectively separate them. The latter experimental results clearly validate the superiority of our joint shape and texture detection. Although the fusion method might be simple at a glance, this is exactly the strength of our approach: a simple fusion method already worked far better than previous non-fusion approaches.

3 Haar of Oriented Gradients

To effectively capture both shape and texture information, we propose a set of new features based on oriented gradients.

3.1 Oriented gradients features

Given the image I, the image gradient $\overrightarrow{g}(x) = \{g_h, g_v\}$ for the pixel x is computed as:

$$g_h(x) = G_h \otimes I(x), \quad g_v(x) = G_v \otimes I(x), \tag{1}$$

where G_h and G_v are horizontal and vertical filters, and $\otimes$ is convolution operator. A bank of oriented gradients $\{g_o^k\}_{k=1}^K$ are constructed by quantifying the gradient $\overrightarrow{g}(x)$ on a number of K orientation bins:

$$g_o^k(x) = \begin{cases} |\overrightarrow{g}(x)| & \theta(x) \in \text{bin}_k \\ 0 & \text{otherwise} \end{cases}, \tag{2}$$

where $\theta(x)$ is the orientation of the gradient $\overrightarrow{g}(x)$. We call the image g_o^k *oriented gradients channel*. Figure 4 shows the oriented gradients on a cat head image. In this example, we quantify the orientation into four directions. We also denote the sum of oriented gradients of a given rectangular region R as:

$$S^k(R) = \sum_{x \in R} g_o^k(x). \tag{3}$$

It can be very efficiently computed in a constant time using integral image technique [18].

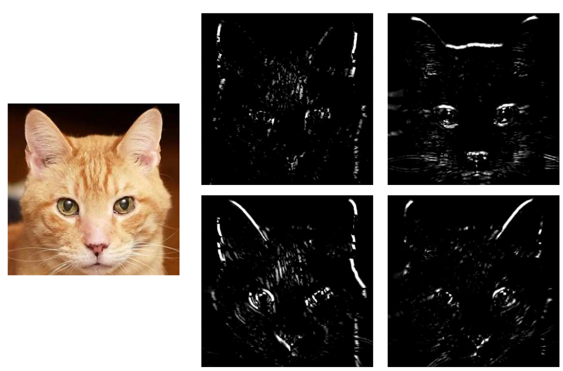

Fig. 4. Oriented gradients channels in four directions.

Since the gradient information at an individual pixel is limited and sensitive to noise, most of previous works aggregate the gradient information in a rectangular region to form more informative, mid-level features. Here, we review two most successful features: HOG and EOH.

HOG-cell. The basis unit in the HOG descriptor is the weighted orientation histogram of a "cell" which is a small spatial region, e.g., 8×8 pixels. It can be represented as:

$$\text{HOG-cell}(R) = [S^1(R), ..., S^k(R), ..., S^K(R)]. \quad (4)$$

The overlapped cells (e.g., 4×4) are grouped and normalized to form a larger spatial region called "block". The concatenated histograms form the HOG descriptor.

In Dalal and Triggs's human detection system [1], a linear SVM is used to classify a 64×128 detection window consisting of multiple overlapped 16×16 blocks. To achieve near real-time performance, Zhu et al. [21] used HOGs of variable-size blocks in the boosting framework .

EOH. Levi and Weiss [7] proposed three kinds of features on the oriented gradients:

$$\text{EOH}_1(R, k1, k2) = (S^{k_1}(R) + \epsilon)/(S^{k_2}(R) + \epsilon),$$
$$\text{EOH}_2(R, k) = (S^k(R) + \epsilon)/(\textstyle\sum_j (S^j(R) + \epsilon)),$$
$$\text{EOH}_3(R, \overline{R}, k) = (S^k(R) - S^k(\overline{R}))/sizeof(R),$$

where $\overline{R}$ is the symmetric region of R with respect to the vertical center of the detection window, and ϵ is a small value for smoothing. The first two features capture whether one direction is dominative or not, and the last feature is used to find symmetry or the absence of symmetry. Note that using EOH features only may be insufficient. In [7], good results are achieved by combining EOH features with Haar features on image intensity.

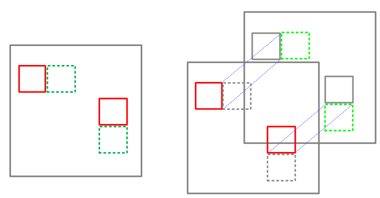

Fig. 5. Haar of Oriented Gradients. Left: in-channel features. Right: orthogonal features.

3.2 Our features - Haar of Oriented Gradients

In face detection, the Haar features demonstrated their great ability to discover local patterns - intensity difference between two subregions. But it is difficult to find discriminative local patterns on the cat head which has more complex and subtle fine scale textures. On the contrary, the above oriented gradients features mainly consider the marginal statistics of gradients in a single region. It effectively captures fine scale texture orientation distribution by pixel level edge detection operator. However, it fails to capture local spatial patterns like the Haar feature. The relative gradient strength between neighboring regions is not captured either.

To capture both the fine scale texture and the local patterns, we need to develop a set of new features combining the advantage of both Haar and gradient features. Taking a close look at Figure 4, we may notice many local patterns in each oriented gradients channel which is sparser and clearer than the original image. We may consider that the gradient filter separates different orientation textures and pattern edges into several channels thus greatly simplified the pattern structure in each channel. Therefore, it is possible to extract Haar features from each channel to capture the local patterns. For example, in the horizontal gradient map in Figure 4, we see that the vertical textures between the two eyes are effectively filtered out so we can easily capture the two eye pattern using Haar features. Of course, in addition to capturing local patterns within a channel, we can also capture more local patterns across two different channels using Haar like operation. In this paper, we propose two kinds of features as follows:

In-channel features:

$$\text{HOOG}_1(R_1, R_2, k) = \frac{S^k(R_1) - S^k(R_2)}{S^k(R_1) + S^k(R_2)}. \tag{5}$$

These features measure the relative gradient strength between two regions R_1 and R_2 in the same orientation channel. The denominator plays a normalization role since we do not normalize $S^k(R)$.

Orthogonal-channel features:

$$\text{HOOG}_2(R1, R2, k, k^*) = \frac{S^k(R_1) - S^{k^*}(R_2)}{S^k(R_1) + S^{k^*}(R_2)}, \tag{6}$$

where k^* is the orthogonal orientation with respect to k, i.e., $k^* = k + K/2$. These features are similar to the in-channel features but operate on two orthogonal channels. In theory, we can define these features on any two orientations. But we decide to compute only the orthogonal-channel features based on two considerations: 1) orthogonal channels usually contain most complementary information. The information in two channels with similar orientations is mostly redundant; 2) we want to keep the size of feature pool small. The AbaBoost is a sequential, “greedy” algorithm for the feature selection. If the feature pool contains too many uninformative features, the overall performance may be hurt. In practice, all features have to be loaded into the main memory for efficient training. We must be very careful about enlarging the size of features.

Considering all combinations of R_1 and R_2 will be intractable. Based on the success of Haar features, we use Haar patterns for R_1 and R_2, as shown in Figure 5. We call the features defined in (5) and (6), Haar of Oriented Gradients (HOOG).

4 Experimental Results

4.1 Data set and evaluation methodology

Our evaluation data set includes two parts, the first part is our own data, which includes 10,000 cat images mainly obtained from flickr.com; the second part is from PASCAL 2007 cat data, which includes 679 cat images. Most of our own cat data are near frontal view. Each cat head is manually labeled with 9 points, two for eyes, one for mouth, and six for ears, as shown in Figure 6. We randomly divide our own cat face images into three sets: 5,000 for training, 2000 for validation, and 3,000 for testing.We follow the PASCAL 2007 original separations of training, validation and testing set on the cat data. Our cat images can be downloaded from http://mmlab.ie.cuhk.edu.hk/ for research purposes.

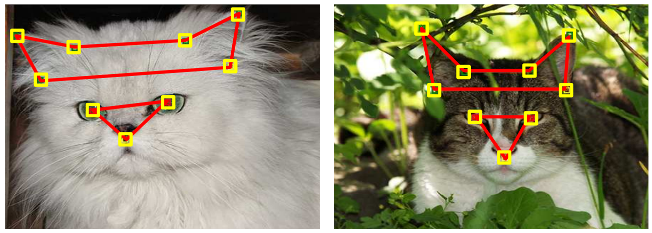

Fig. 6. The cat head image is manually labeled by 9 points.

We use the evaluation methodology similar to PASCAL challenge for object detection. Suppose the ground truth rectangle and the detected rectangle are r_g and r_d, and the area of those rectangles are A_g and A_d. We say we correctly detect a cat head only when the overlap of r_g and r_d is larger than 50%:

$$D(r_g, r_d) = \begin{cases} 1 & \text{if } \frac{(A_g \cap A_d)}{(A_g \cup A_d)} > 50\% \ , \\ 0 & \text{otherwise} \end{cases} , \tag{7}$$

where $D(r_g, r_d)$ is a function used to calculate detection rate and false alarm rate.

4.2 Implementation details

Training samples. To train the shape detector, we align all cat head image with respect to ears. We rotate and scale the image so that two tips of ears appear on a horizontal line and the distance between two tips is 36 pixel. Then, we extract a 48×48 pixel region, centered 20 pixels below two tips. For the texture detector, a 32×32 pixel region is extracted. The distance between two eyes is 20 pixel. The region is centered 6 pixel below two eyes.

Features. We use 6 unsigned orientations to compute the oriented gradients features. We find the improvement is marginal when finer orientations are used. The horizontal and vertical filters are $[-1, 0, 1]$ and $[-1, 0, 1]^T$. No thresholding is applied on the computed gradients. For both shape and texture detector, we construct feature pools with 200,000 features by quantifying the size and location of the Haar templates.

4.3 Comparison of features

First of all, we compare the proposed HOOG features with Haar, Haar + EOH, and HOG features on both shape detector and texture detector using our Flickr cat data set. For the Haar features, we use all four kinds of Haar templates. For the EOH features, we use default parameters suggested in [7]. For the HOG features, we use 4×4 cell size which produces the best results in our experiments.

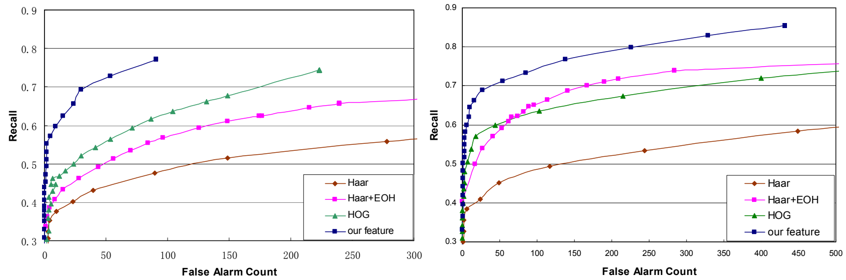

(a) shape detector (b) texture detector

Fig. 7. Comparison of Haar, Haar+EOH, HOG, and our features.

Figure 7 shows the performances of the four kinds of features. The Haar feature on intensity gives the poorest performance because of large shape and texture variations of the cat head. With the help of oriented gradient features, Haar + EOH improves the performance. As one can expect, the HOG features perform better on the shape detector than on the texture detector. Using both in-channel and orthogonal-channel information, the detectors based on our features produce the best results.

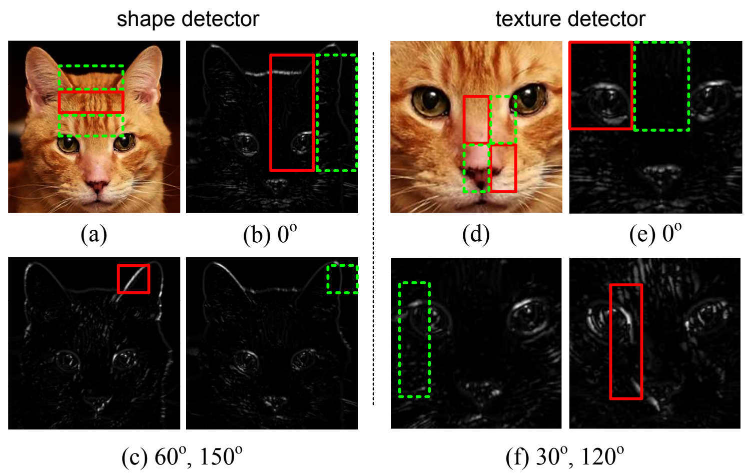

Fig. 8. Best features leaned by the AdaBoost. Left (shape detector): (a) best Haar feature on image intensity. (b) best in-channel feature. (c) best orthogonal feature on orientations 60^o and 150^o. Right (texture detector): (d) best Haar feature on image intensity. (e) best in-channel feature. (f) best orthogonal-channel feature on orientations 30^o and 120^o.

In Figure 8, we show the best in-channel features in (b) and (e), and the best orthogonal-channel features in (c) and (f), learned by two detectors. We also show the best Haar features on image intensity in Figure 8 (a) and (d). In both detectors, the best in-channel features capture the strength differences between a region with strongest horizontal gradients and its neighboring region. The best orthogonal-channel features capture the strength differences in two orthogonal orientations.

In the next experiment we investigate the role of in-channel features and orthogonal-channel features. Figure 9 shows the performances of the detector using in-channel features only, orthogonal-channel features only, and both kinds of features. Not surprisingly, both features are important and complementary.

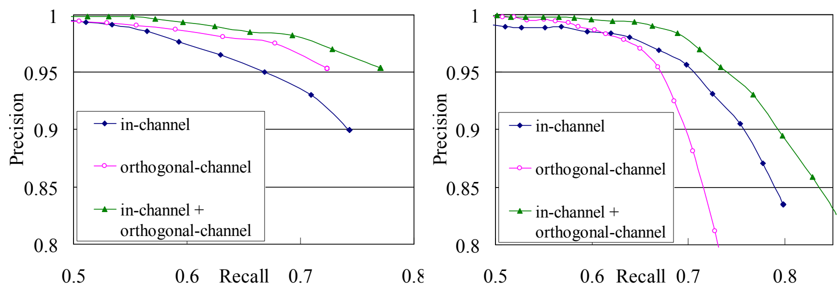

(a) shape detector (b) texture detector

Fig. 9. The importance of in-channel features and orthogonal-channel features.

4.4 Joint shape and texture detection

In this sub-section, we evaluate the performance of the joint fusion on the Flickr cat data. To demonstrate the importance of decomposing shape and texture features, we also train a cat head detector using training samples aligned by an optimal rotation+scale transformation for the comparison. Figure 10 shows four ROC curves: a shape detector, a texture detector, a head detector using optimal transformation, and a joint shape and texture fusion detector. Several important observations can be obtained: 1) the performance of fusion detector is substantially improved! For a given total false alarm count 100, the recall is improved from 0.74/0.75/0.78 to 0.92. Or the total false alarm is reduced from 130/115/90 to 20, for a fixed recall 0.76. In image retrieval and search applications, it is a very nice property since high precision is preferred; 2) the head detector using optimal transformation does not show superior performance. The discriminative abilities of both shape and texture features are decreased by the optimal transformation; 3) the maximal recall value of the fusion detector (0.92) is larger than the maximal recall values of three individual detectors(0.77/0.82/0.85). This shows the complementary abilities of two detectors - one detector can find many cat heads which is difficult to the other detector; 4) note that the curve of fusion detector is very steep in the low false alarm region, which means the fusion detector can effectively improve the recall while maintain a very low false alarm rate.

The superior performance of our approach verifies a basic idea in object detection – context helps! The fusion detector finds surrounding evidence to verify the detection result. In our cat head detection, when the shape detector reports a cat, the fusion detector checks the surrounding shape information. If the texture detector says it may be a cat, we increase the probability to accept this cat. Otherwise, we decrease the probability to reject this cat.

Figure 12 gives some detection examples having variable appearance, head shape, illumination, and pose.

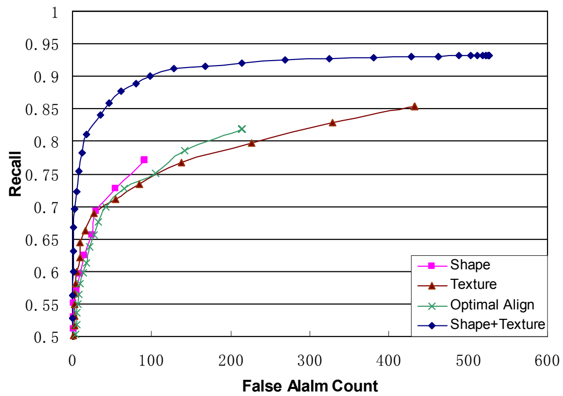

Fig. 10. Joint shape and texture detection.

4.5 Experiment on the PASCAL 2007 cat data

We also evaluate the proposed approach on the PASCAL 2007 cat data [2]. There are two kinds of competitions for the detection task: 1) Competition 3 - using both training and testing data from PASCAL 2007; 2) Competition 4 - using arbitrary training data. Figure 11 (a) shows the precision-recall curves of our approach and the best reported method [2] on Competition 3. We compute the Average Precision (AP) as in [2] for a convenient comparison. The APs of our approach and the best reported method is 0.364 and 0.24, respectively. Figure 11(b) shows the precision-recall curves on Competition 4. Since there is no reported result on Competition 4, we compare our approach with the detectors using Haar, EOH, and HoG respectively. All detectors are trained on the same training data. The APs of four detectors (ours, HOG, Haar+EOH, Harr) are 0.632, 0.427, 0.401, and 0.357. Using larger training data, the detection performance is significantly improved. For example, the precision is improved from 0.40 to 0.91 for a fixed recall 0.4. Note that the PASCAL 2007 cat data treat the whole cat body as the object and only small fraction of the data contain near frontal cat face. However, our approach still achieves reasonable good results (AP=0.632) on this very challenging data (the best reported method's AP=0.24).

5 Conclusion and Discussion

In this paper, we have presented a cat head detection system. We achieved excellent results by decomposing texture and shape features firstly and fusing detection results secondly. The texture and shape detectors also greatly benefit from a set of new oriented gradient features. Although we focus on the cat head detection problem in this paper, our approach can be extended to detect other categories of animals. In the future, we are planing to extend our approach to multi-view cat head detection and more animal categories. We are also interest in exploiting other contextual information, such as the presence of animal body, to further improve the performance.

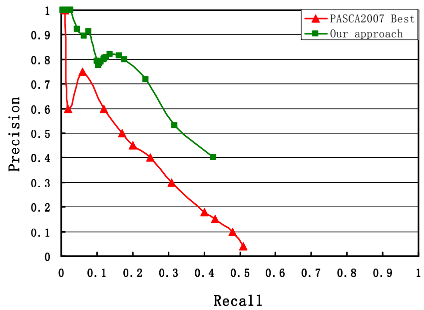

(a) Competition 3

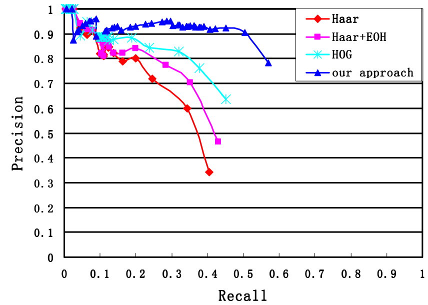

(b) Competition 4

Fig. 11. Experiments on PASCAL 2007 cat data. (a) our approach and best reported method on Competition 3 (specified training data). (b) four detectors on Competition 4 (arbitrary training data).

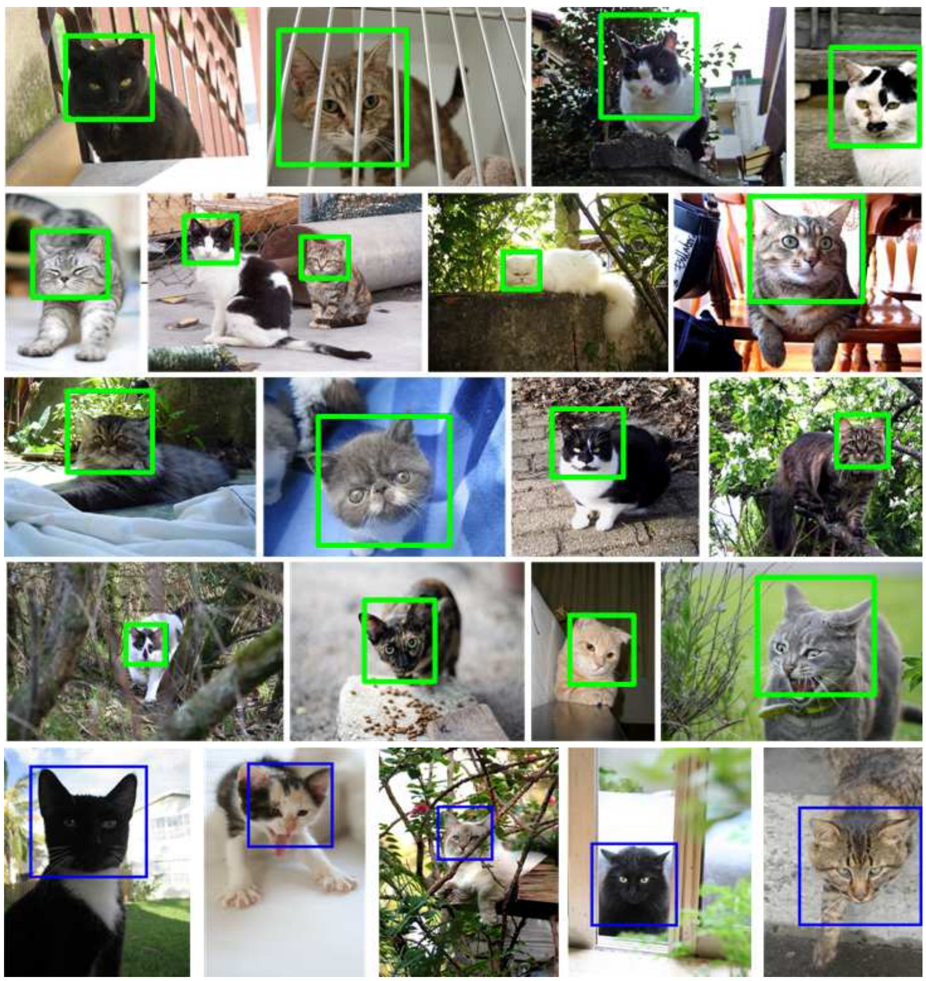

Fig. 12. Detection results. The bottom row shows some detected cats in PASCAL 2007 data.

References

1. Navneet Dalal and Bill Triggs. Histograms of oriented gradients for human detection. In *CVPR*, volume 1, pages 886–893, 2005.
2. Mark Everingham, Luc van Gool, Chris Williams, John Winn, and Andrew Zisserman. The PASCAL Visual Object Classes Challenge 2007 (VOC2007) Results. http://www.pascal-network.org/challenges/VOC/voc2007/workshop/index.html.
3. Pedro F. Felzenszwalb. Learning models for object recognition. In *CVPR*, volume 1, pages 1056–1062, 2001.
4. Dariu M. Gavrila and Vasanth Philomin. Real-time object detection for smart vehicles. In *CVPR*, volume 1, pages 87–93, 1999.
5. Bernd Heisele, Thomas Serre, Massimiliano Pontil, and Tomaso Poggio. Component-based face detection. In *CVPR*, volume 1, pages 657–662, 2001.
6. Bastian Leibe, Edgar Seemann, and Bernt Schiele. Pedestrian detection in crowded scenes. In *CVPR*, volume 1, pages 878–885, 2005.
7. Kobi Levi and Yair Weiss. Learning object detection from a small number of examples: the importance of good features. In *CVPR*, volume 2, pages 53–60, 2004.
8. David G. Lowe. Object recognition from local scale-invariant features. In *ICCV*, volume 2, pages 1150–1157, 1999.
9. Krystian Mikolajczyk, Cordelia Schmid, and Andrew Zisserman. Human detection based on a probabilistic assembly of robust part detectors. In *ECCV*, volume 1, pages 69–82, 2004.
10. Anuj Mohan, Constantine Papageorgiou, and Tomaso Poggio. Example-based object detection in images by components. *IEEE Trans. Pattern Anal. Machine Intell.*, 23(4):349–361, April 2001.
11. Stefan Munder and Dariu M. Gavrila. An experimental study on pedestrian classification. *IEEE Trans. Pattern Anal. Machine Intell.*, 28(11):1863–1868, November 2006.
12. Constantine Papageorgiou and Tomaso Poggio. A trainable system for object detection. *Intl. Journal of Computer Vision*, 38(1):15–33, 2000.
13. Remi Ronfard, Cordelia Schmid, and Bill Triggs. Learning to parse pictures of people. In *ECCV*, volume 4, pages 700–714, 2004.
14. Henry A. Rowley, , Shumeet Baluja, and Takeo Kanade. Neural network-based face detection. *IEEE Trans. Pattern Anal. Machine Intell.*, 20(1):23–38, 1998.
15. Payam Sabzmeydani and Greg Mori. Detecting pedestrians by learning shapelet features. In *CVPR*, 2007.
16. Henry Schneiderman and Takeo Kanade. A statistical method for 3d object detection applied to faces and cars. In *CVPR*, volume 1, pages 746–751, 2000.
17. Oncel Tuzel, Fatih Porikli, and Peter Meer. Human detection via classification on riemannian manifolds. In *CVPR*, 2007.
18. Paul Viola and Michael J. Jones. Robust real-time face detection. *Intl. Journal of Computer Vision*, 57(2):137–154, May 2004.
19. Bo Wu and Ram Nevatia. Detection of multiple, partially occluded humans in a single image by bayesian combination of edgelet part detectors. In *ICCV*, volume 1, pages 90–97, 2005.
20. Rong Xiao, Huaiyi Zhu, He Sun, and Xiaoou Tang. Dynamic cascades for face detection. In *ICCV*, volume 1, pages 1–8, 2007.
21. Qiang Zhu, Shai Avidan, Mei-Chen Yeh, and Kwang-Ting Cheng. Fast human detection using a cascade of histograms of oriented gradients. In *CVPR*, volume 2, pages 1491–1498, 2006.